Int. J. Electrochem. Sci., 3 **(2008)** 29 - 43

International Journal of ELECTROCHEMICAL SCIENCE
www.electrochemsci.org

Pitting Corrosion of Tin by Acetate Anion in Acidic Media

Hamdy H. Hassan[1,*] *, Khalid Fahmy*[2]

[1] Chemistry Department, Faculty of Science, Ain Shams University, Cairo-11566, Egypt
[2] Chemistry Department, Faculty of Science, King Khaled University, Abha, KSA
[*]E-mail: hamdihh@hotmail.com , present address: King Khaled University, Abha, KSA

Received: 2 October 2007 / *Accepted:* 30 October 2007 / *Online published:* 20 November 2007

The corrosion behaviour of tin is studied in acetate buffer solutions (pH 4.5). The potentiodynamic anodic polarization curve in 0.1M acetate solution exhibits two anodic peaks A1 and A2 prior to the passive layer formation region which is followed by pitting corrosion. A1 and A2 are attributed to stannous and stannic species formation. The effect of scan rate on the potentiodynamic behaviour of tin in this solution was studied. It showed that the corrosion process in the potential range of peaks A1 and A2 is mass transport controlled. Pitting corrosion is confirmed by light microscope images. The negative going scans of the cyclic voltammograms show three cathodic peaks C1, C2 and C3. The potentiostatic current time transients, at different electrolyte concentrations and applied potentials (around the pitting potential) involve three stages. The first stage, in which current decreases rapidly with time till reaching a minimum value i_m at the incubation time t_i . The second and third stages, where current increases again linearly with time at two different slopes, are correlated to the pit nucleation and growth respectively. The nucleation rate (t_i^{-1}) was found to increase with increasing the electrolyte concentration and the anodic applied potential. The impedance spectra, at potentials of passive layer and pitting formations, exhibit a high frequency conductive semicircle and a low frequency inductive loop. The results showed a decrease in the electrode impedance as the applied potential approached the pitting potential.

Keywords: Acetate, pitting , tin, EIS, chronoamperometry

1. INTRODUCTION

Tin is widely employed in the manufacture of food containers and its electrochemical behaviour in the presence of organic acids has attracted considerable interest [1-6]. In most cases the anodic dissolution of tin in these acids exhibits active/passive behaviour. In the active dissolution region in acid media, tin dissolves as Sn^{2+} which easily oxidized to Sn^{4+} [2,5,7]

$$Sn = Sn^{2+} + 2e^- \quad (1)$$

$$Sn^{2+} = Sn^{4+} + 2e^- \quad (2)$$

Consequently, Sn^{4+} hydrolyze in acid media forming the highly insoluble $Sn(OH)_4$ [8,9] which precipitates on the surface giving rise to a passive film.

$$Sn^{4+} + 4H_2O = Sn(OH)_4 + 4\ H^+ \quad (3)$$

The stability of the passive film increases with its irreversible dehydration to SnO_2 [2,6,8]

$$Sn(OH)_4 = SnO_2.H_2O + H_2O \quad (4)$$

Non of the studied acids cause pitting corrosion of tin metal without the addition of aggressive anions. However, our preliminary experiments indicates the aggressive action of acetate anion towards the passive film formed on tin. Several papers have reported an increase in the rate of corrosion of the steel when acetate ion (or the anions of other weak acids) is also present in the CO_2 saturated sodium chloride brine [10-12].

The aim of this work is to study in some details the pitting corrosion of tin metal provoked by the acetate anion in different experimental conditions. In addition to the practical importance of this study, it has also academic value. As a result of this work we can count the acetate ion among the aggressive anion that may cause pitting corrosion of some metals.

2. EXPERIMENTAL PART

The experiments were carried out in 0.01- 0.5 M acetate buffers (pH~ 4.5 ± 0.1). Equal volumes of *x*M sodium acetate and acetic acid were mixed to prepare *x*M of the working solutions. All solutions were prepared from analytical grade chemicals and doubly distilled water. The working electrode was a tin rod (99.998%; Sigma Aldrich), its apparent exposed surface area was 0.2 cm^2. The counter electrode was a platinum wire. The working electrode potentials were recorded vs. a silver-silver chloride electrode (Ag/AgCl). Prior to each experiment, the working electrode was successively polished with finest grade emery papers, degreased with acetone and washed with running doubly distilled water and finally dried with filter paper. The electrode was then immediately immersed in the test solution. All measurements were carried out at room temperature ($25 \pm 1\ ^{\circ}C$).

The potentiodynamic polarization (E/i) curves were recorded by changing the electrode potential automatically from -1.25 V to the desired anodic potential limit, E_a, with a scan rate of 30 mVs^{-1}. The tin surface was photomicrographed with BUEHLER ViewMet Inverted Metallographic Microscope connected with a µEye digital camera. Photos were taken before and after the electrode polarization at E = 1.0 V for 5 min. in a 0.1 M acetate buffer solution. The anodic current transients at constant anodic potentials E_a were recorded for 120 seconds.

Electrochemical impedance spectroscopy (EIS) measurements were carried out using AC signals of amplitude 5 mV peak to peak at different conditions in the frequency range of 10 kHz to 50

mHz. An Autolab Potentiostat/Galvanostat (PGSTAT30) with FRA2 module and a personal computer were used to perform the above mentioned techniques. The GPES and FRA (ver. 4.9) software provided by Autolab was utilized in our measurements and fitting processes.

3. RESULTS AND DISCUSSION

3.1. Cyclic voltammetry

Fig (1) shows a typical voltammogram of tin electrode in 0.1 M acetate buffer. The electrode was staying for 60 s at -1.25 V then the potential was swept from -1.25 V up to 1.2 V with a scan rate of 30 mVs^{-1}. It is clear from this figure that, on the positive going sweep, the cathodic current density decreases gradually forming a small cathodic current plateau (P1) just before the corrosion potential. This plateau corresponds to hydrogen evolution reaction on the tin surface. Studies performed in systems containing $HOAc/OAc^-$ have suggested that the corrosion mechanism takes place through the adsorption of HOAc on the metallic surface [13]. It is generally accepted that hydrogen evolution in acetate buffers occurs via the parallel reduction of the free proton and the acetic acid (equations (5) and (6)) [14]; the latter reaction occurs via the fast dissociation of the acetic acid (with rate constant of ~ 10^6 s^{-1}) [15], followed by the reduction of the librated proton, equation (6).

$$H^+ + e^- \rightarrow \tfrac{1}{2} H_2 \qquad (5)$$

$$HOAc \xleftarrow{\text{fast}} H^+ + OAc^- \xrightarrow{e^-} {}_{1/2}H_2 + OAc^- \qquad (6)$$

The electrode reaction in this potential range was proved to follow equation (6) which is fully controlled by the diffusion of HOAc [14].

Behind the corrosion potential, the voltammogram shows an active-passive behaviour. The active dissolution region involves two anodic current peaks A1 and A2, corresponding to the stepwise oxidation of Sn to Sn^{4+} according to equations (1) and (2), respectively. When the surface is completely covered with $Sn(OH)_4$ and/or $SnO_2.H_2O$ film, the dissolution current falls to a small passive current density (i_{pass}), indicating the onset of passivation. However, when the anodic potential exceeds a certain value, the current rises suddenly to a very high value, suggesting breakdown of the passive film and initiation of pitting corrosion. The potential at which the sudden current rise takes place is known as the pitting potential (E_{pit}). The pitting corrosion beyond E_{pit} is confirmed by the light microscope image of the tin surface before and after its polarization at E = 1.0 V (> E_{pit}) for 5 min. in a 0.1M acetate solution (Fig. 2).

The breakdown of the passive film could be ascribed to the relative fast adsorption of OAc^- anions on the passive film [16]. The adsorbed anions create an electric field across the film/electrolyte interface [17]. When the field reaches a certain value, the adsorbed anions succeed to incorporate and penetrate the passive film at local defect points. When the penetrated OAc^- ions reach the substrate, they promote local anodic dissolution, involving the formation of soluble tin acetates and results in pit nucleation.

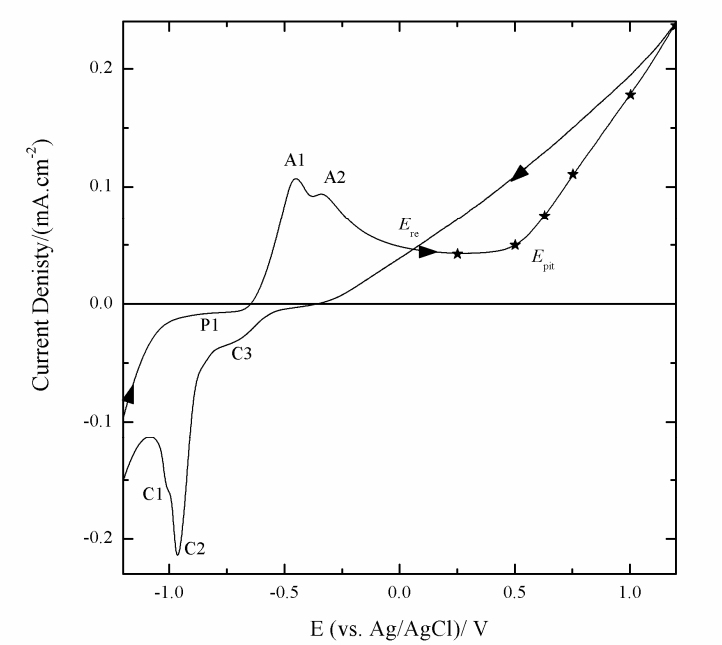

Figure 1. Cyclic voltammogram of tin electrode in 0.1 M acetate solution. The stars on the curve represents the potential values at which impedance plots were recorded in Fig. 10.

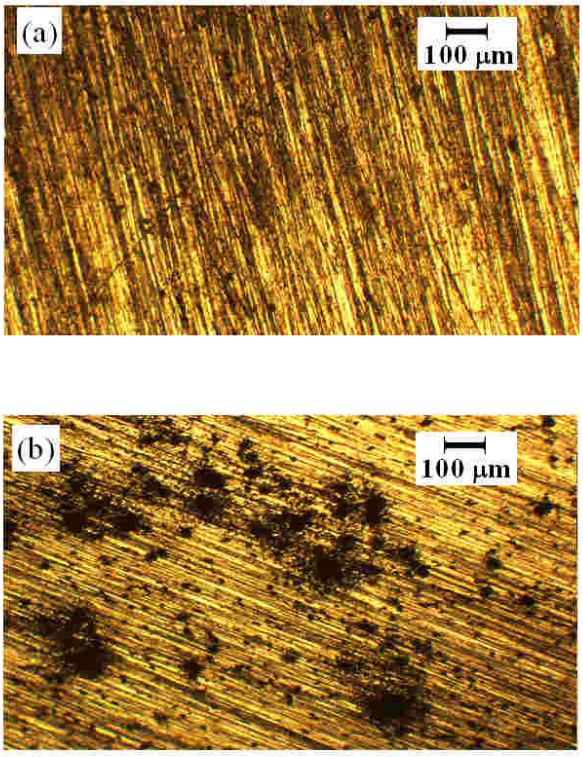

Figure 2. Light microscope images of the tin surface (a) before and (b) after polarization at E = l.0 V in a 0.1M acetate buffer solution for 5 min.

On reversing the sweep, a hysteresis loop is formed which is a characteristic of pitting corrosion phenomenon [18-20]. This hysteresis loop allows the repassivation potential *E*rp to be determined. *E*rp represents the potential value below which no pitting occurs and above which pit nucleation starts [19,20]. At more cathodic potentials, three cathodic current peaks (C1, C2, C3) are formed. It is important to establish the relationship between these cathodic peaks and the corresponding anodic processes, which take place over various ranges of potential in the anodic sweep. For this reason, experiments were performed by progressively increasing the upper anodic potential limit, E_a, at which successive anodic sweeps were reversed, Fig.3. It is clear from this figure that reversal of the sweep in the potential range of the cathodic plateau P1 gives rise to the reduction peak C1 (curve 1). Therefore, it is likely that peak C1 is related to the reduction of the adsorbed HOAc. The cathodic peak C3 is observed, if the anodic sweep is reversed within the potential range of A1 (curves 2 and 3). Thus it can be assigned to the electro-reduction of the corrosion product formed in this range (the free Sn^{2+} and/or Sn^{4+} ions). It is worth noting that the charge of this peak increase and its peak potential shifts to more negative values as E_a value becomes more anodic (curves 4-7). In other words, as the vertex potential shifts more anodic in the passive region the cathodic peak C3 gradually vanishes and the more cathodic C2 peak regularly appears. Consequently, the cathodic peak C2 may be attributed to the reduction of the passive layer ($Sn(OH)_4$ and/or SnO_2) formed during the anodic sweep. When the anodic sweep is reversed after the pitting potential, $E_a > E_{pit}$, pitting corrosion commences leading to the dissolution of a bare metal within the pits. The small cathodic peak C3 reappears as a result of reducing the free Sn ions formed through the pits. The height of this peak increase as E_a moves away from E_{pit} (curves 8-10).

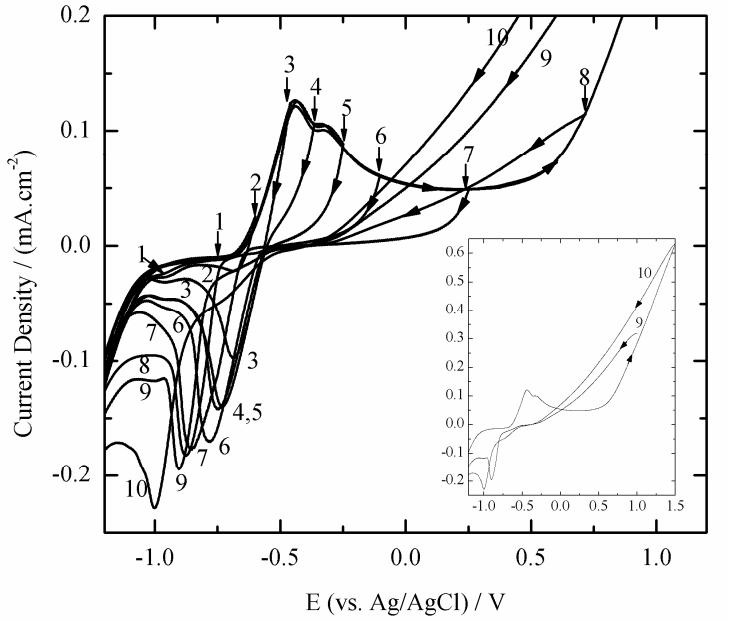

Figure 3. The effect of increasing the upper anodic vertex potential limit, E_a, on the cyclic voltammograms of tin in 0.1 M acetate buffer. The insert is a zooming out for curves 9, 10.

Fig.4 illustrates the influence of the number of successively repeated cycling on the general feature of the voltammogram of tin electrode in 0.1 M acetate buffer between –1.25 V and 1.2 V at 30 mVs^{-1}. The results infer that upon successive cycling, the pitting potential E_{pit} shifts to more anodic values i.e. the passive layer becomes more protective. Consequently, a marked decrease is observed in the heights of the cathodic peak C2 and C3, which are related to the reduction of the passive layer and pitting corrosion product (Sn^{2+} and/or Sn^{4+}) formed during the anodic half cycle in the potential regions before and after E_{pit}, respectively. In addition, the heights of the anodic peaks A1 and A2 are also decreased with successive cycling. This is related to the incomplete reduction of the formed passive layers during the previous cathodic half cycles.

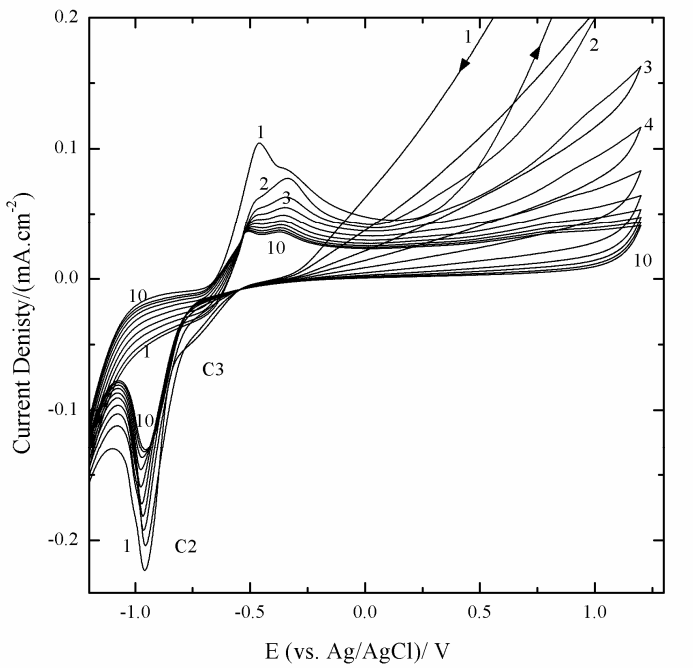

Figure 4. Effect of repetitive cycling upon voltammograms of tin in 0.1 M acetate buffer between -1.25 V and 1.2 V with scan rate of 30 mVs^{-1}. The integers indicate cycle number.

Fig. 5 shows the effect of scan rate on the voltammograms of the tin electrode in 0.1 M acetate buffer. It is seen that the current density of the anodic peaks A1 and A2 increase and their peaks potentials shift to more anodic values with increasing the sweep rate. The plot of peaks currents vs. $\nu^{1/2}$ gives straight lines. The line of peak A2 passes through the origin while that of A1 meet the current axis at a positive current value (Fig.6a). These results suggest that tin oxidation processes within the potential range of peak A1 is mixed controlled process while those occurred in the potential range of A2 is mainly diffusion controlled.

For a pure diffusion controlled process under potentiodynamic conditions, the slope of the linear relation of i_{peak} vs $\nu^{1/2}$ is proportional to the concentration of the diffusing species (C) and to the square root of its diffusion coefficient (D) according to the following equation [21]:

$$i_{peak} = \alpha \beta z^{1/2} D^{1/2} C \nu^{1/2} \qquad (7)$$

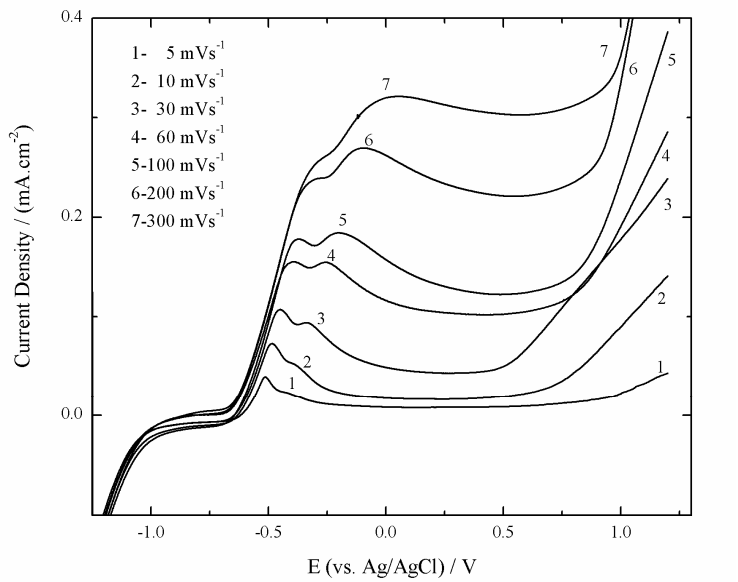

Figure 5. The effect of scan rate on the potentiodynamic anodic polarization curve of tin electrode in in 0.1 M acetate buffer (pH 4.5).

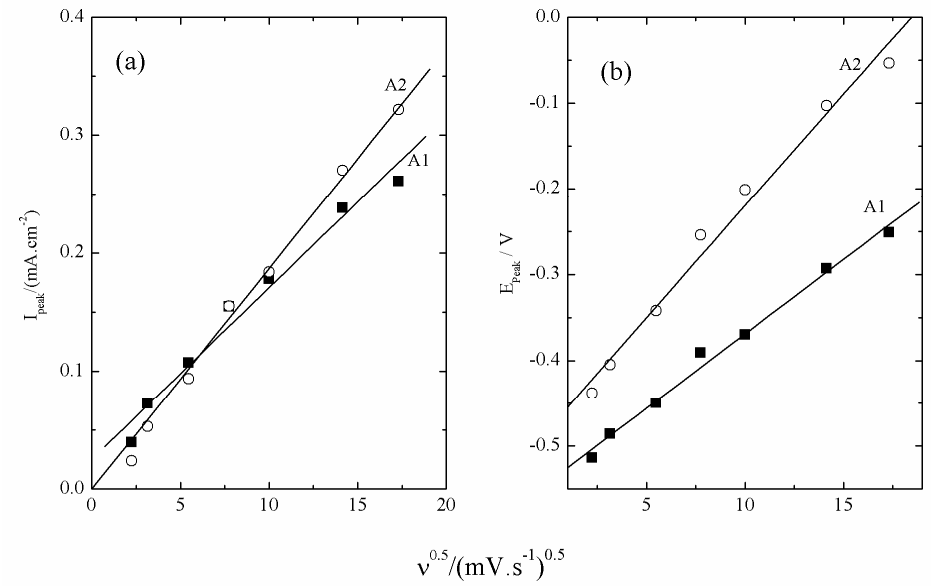

Figure 6. Linear dependence of peaks currents (a) and potentials (b) on the square root of the scan rate for tin electrode. Data were obtained from Fig. 5.

where α and β are constants and (z) is the number of exchanged electrons. It is worth noting that the relative height of peaks A1 and A2 depends greatly on the scan rate. At slow scans the current density of A1 exceeds that of A2. However, increasing the scan rate affects the current of the diffusion controlled A2 more than that of the mixed controlled A1 to the extent that A2 becomes higher than A1 at fast scans. Moreover, the linear behaviour of both of the peak currents and potentials with the square root of the scan rate is in accordance with Müller and Calanddra`s model [4,22,23], Fig. 6. As stated by the authors, the film formation is related to the reaction products which cover the electrode surface,

increasing the ohmic resistance in the pores of the film. On the other hand, E_{pit} shifts to more cathodic values with increasing ν, however at ν>30 mVs^{-1}, it shifts in the positive direction with increasing ν. The latter trend has been interpreted in terms of incubation time [24].

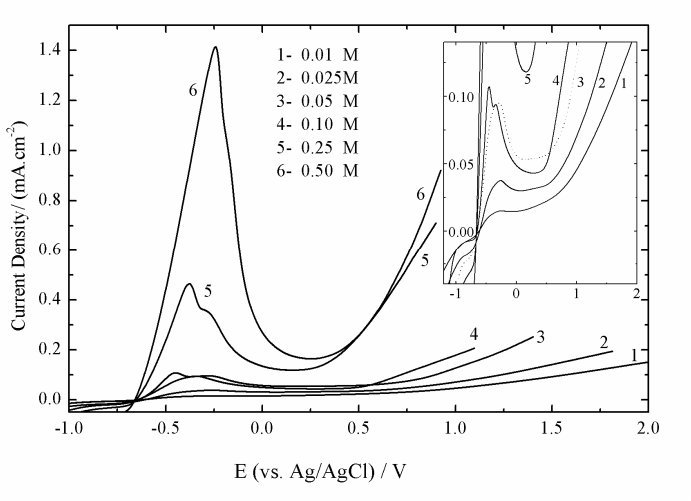

Figure 7. Potentiodynamic anodic polarization curves of tin electrode in acetate buffer solutions of different concentrations (pH~4.5) at a scan rate of 30 mVs^{-1}. The insert is zooming up for curves 1-4.

Figure 7 illustrates the influence of acetate buffer concentration (0.01 to 0.5 M) at pH 4.5 on the voltammograms of tin at 30 mVs^{-1}. The results display that an increase in solution concentration increases the anodic peaks current density and shifts their peak potentials to more positive value as a result of increasing the rate of tin corrosion. Likewise, the passive current also increases with increasing the electrolyte concentration and the pitting potential E_{pit} shifts to more negative values with increasing the solution concentration. These behaviours may be due to weakening of the passive film as a result of the competition between its formation and the formation of the soluble tin acetate and the increase of the number of aggressive acetate ions that attack the passive layer, respectively.

3.2. Potentiostatic current-time transients

The potentiostatic current-time transients for tin in 0.1 M acetate buffer solution at various potential limits E_a (in the vicinity of E_{pit}) were recorded. Fig. 8 (a) and (b) represent these transients in linear and logarithmic scales, respectively. For all the studied E_a values, the current transient initially decreases to a minimum value i_m at a characteristic pitting time parameter t_i (incubation time). The reciprocal of the incubation time (t_i^{-1}) is taken as the rate of pit nucleation. The initial decrease in the transient current (i) is related to the growth of the passive layer on the electrode surface. The film growth kinetics fits the model proposed by Macdonald et al. [25,26] which can be given by:

$$i = A.t^{-n} \qquad (8)$$

where A and n are constants depending upon the potential limit E_a and the electrolyte concentration. The value of n represents the passive growth rate [27] and is given by the slope of the descending part of the log i–log t relationship (Fig.8b). The data given in Table 1 show that the values of n decreases with increasing the applied potential E_a. This means that as E_a is made more positive the growth rate of the passive layer decreases.

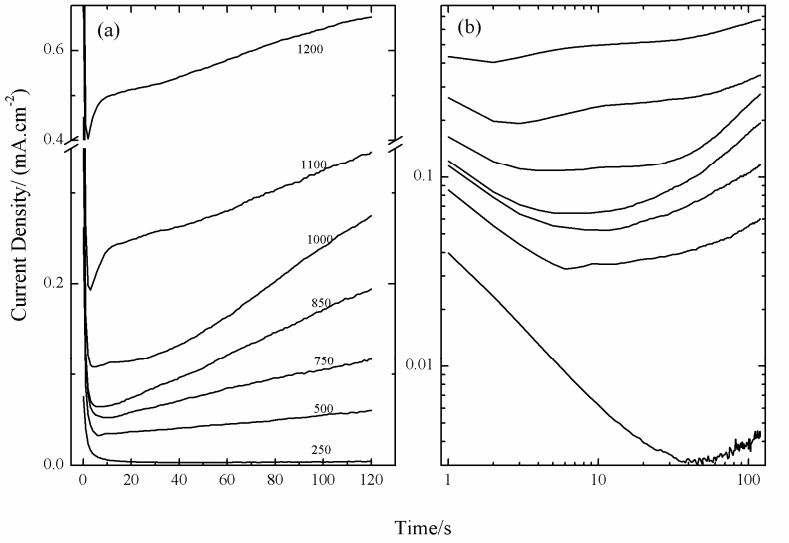

Figure 8. Current-time transient for tin electrode in 0.1 M acetate solution at different applied potential.

Table 1. Effect of applied anodic potential on the kinetic parameters derived from potentiostatic current-time transients for tin in 0.1 M acetate buffer solution (pH 4.5) (Fig.8) for passive layer growth (n), pit nucleation (b_1, t_i^{-1} and i_m) and its growth (b_2)

Potential, E_a/mV	n	b_1	b_2	$(t_i^{-1})/(s^{-1})$	$i_m/(\mu A.cm^{-2})$
250	0.81		0.37	0.023	3.2
500	0.56		0.39	0.123	33.4
750	0.50		0.43	0.130	53.5
825	0.50		0.62	0.148	65.2
1000	0.37	0.07	0.73	0.248	108.4
1100	0.29	0.16	0.30	0.345	192.2
1400	0.10	0.16	0.22	0.503	413.6

After t_i, the current transient increases again exhibiting two straight lines with two different slopes. The time at the inflection point is denoted as induction time (τ). The first straight line may be considered to correspond to the period of pit nucleation while the second line to that of pit growth [28]. The increase of current transient after t_i can be represented by the Engell-Stolica equation for pitting corrosion [29]:

$$i = B.t^b \qquad (9)$$

where B and b are constants depending upon the applied potential and the solution concentration. The slopes of the log i-log t curves after t_i (b_1 for the first line and b_2 for the second line) as well as the pit nucleation rate (t_i^{-1}) and i_m for different potential limit values are given in Table 1. The values of b_2 increases with E_a till the appearance of the first straight line at E_a= 1.0V, then it decreases with time. However, the pit nucleation parameters b_1, (t_i^{-1}) and i_m enhance with the potential limit E_a.

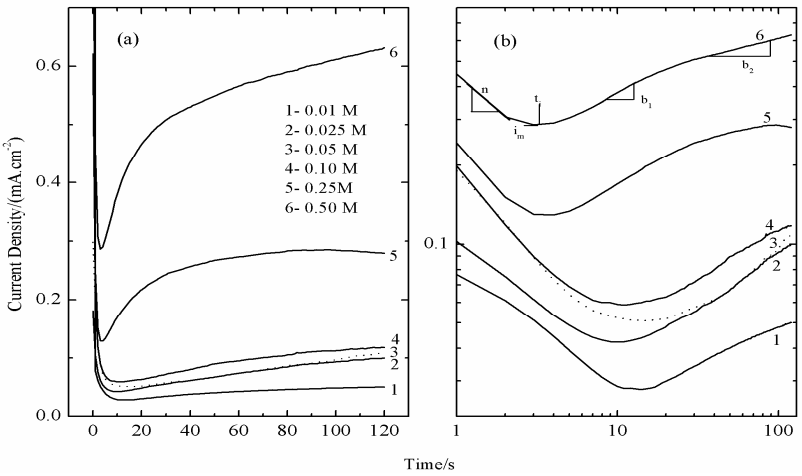

Figure 9. Current-time transient for tin electrode polarized at 900 mV in acetate solution with different concentrations

Table 2. The kinetic parameters derived from potentiostatic current-time transients for Sn in acetate buffer solutions (pH 4.5) with different concentrations at 900 mV (vs. Ag/AgCl) (Fig.9)for passive layer growth (n), pit nucleation (b_1, t_i^{-1} and i_m) and its growth (b2)

Concentration C/M	n	b1	b2	$(t_i^{-1})/(s^{-1})$	$i_m/(\mu A.cm^{-2})$
0.010	0.45		0.32	0.074	27.8
0.025	0.44	0.33	0.44	0.099	42.1
0.050	0.67	0.25	0.57	0.068	51.0
0.100	0.69	0.23	0.32	0.102	59.0
0.250	0.69	0.34	0.18	0.275	129.3
0.500	0.54	0.29	0.15	0.321	288.2

On the other hand, the effect of the solution concentration (pH~4.5) on the potentiostatic current time curves were studied at 900 mV, the results are given in Fig. 9 (a) and (b). The potentiostatic current time curves exhibit the same features described above. The values of n, b_1, b_2, t_i^{-1} and i_m are listed in Table 2 for different electrolyte concentrations. The value of n increases with increasing electrolyte concentration. The values of b_2 increases with concentration till C = 0.05 M. At higher concentrations, b_2 decreases again with time. The values of b_1 are nearly constant while those of b_2, t_i^{-1} and i_m increase with increasing the solution concentration. As the values of E_a and/or the solution concentration increases, the pit nucleation increases. At high values of E_a and C and the

amount of the corrosion product increases to the extent that it re-deposits inside the pits leading to lower pit growth rates. Fig. 2b shows the precipitated corrosion products inside and outside the formed pits.

3.3. Impedance measurements

Fig.10 (a, b) represents the Nyquist plane impedance plots for the tin electrode in 0.1 M acetate buffer at different electrode potentials. The electrode potentials at which impedance measurements were carried out are represented by stars on the voltammogram of Fig. 1. Inspection of Fig 10 (a, b) shows that the presented Nyquist plots consist of charge-transfer semicircle at high frequency (HF) range and an inductive loop at low frequencies (LF) as a result of the presence of adsorbed intermediate species during the dissolution reaction [13,30-32], it may also attributed to the re-dissolution of the passivated surface at low frequencies [33]. The low frequency regions are characterized by a great scattering of the impedance values, which was assigned to an incipient pitting [19,34]. This scattering is limited to lower frequencies at higher anodic potentials. Fig. 10 (c, d) represents respectively the Bode phase angle and impedance magnitude plots recorded for the tin electrode at the same conditions described above. The Bode phase angle plots show single maximum at intermediate frequencies. In addition, a negative phase angle and a slight decrease in the impedance are observed at the low frequency limit denoting the inductive behaviour described above. Consequently, we proposed a one time constant equivalent circuit described in Fig. 10e with a constant phase element, CPE, and an inductive R_L-L loop to fit our data and obtain the different corrosion parameters. The protection layer resistance and the diffuse charge capacitance in it are not separated in this approximation, rather they conceived to be included in this circuit. The impedance of the CPE is expressed as:

$$Z_{CPE} = \frac{1}{Y_0 (j\omega)^n} \qquad (10)$$

where Y_0 is the magnitude of the CPE, $-1 \leq n \leq 1$. The HF loop have depressed semicircular appearance, $0.5 \leq n \leq 1$, which is often referred to as frequency dispersion as a result of the nonhomogeneity [35-37]or the roughness [38] of the solid surface. The HF capacitive loop, R_{ct}-CPE, can be attributed to the charge-transfer reaction.

The impedance at high frequency limit (f = 10 kHz) , R_s, corresponds to the ohmic resistances of the corrosion product films and the solution enclosed between the working electrode and the reference electrode. The intercept of the extrapolation of the charge-transfer semicircle with the real axis in the low frequency range, in Nyquist plots, gives the charge transfer resistance, R_{ct}. The values of R_s and R_{ct} can be derived from Bode impedance plots at high and low frequencies, respectively. Their values and the other equivalent circuit parameters, which obtained from the fitting processes, are represented in Table 3. The values of R_s are nearly constant, while those of R_{ct} decreases drastically with potential as a result of the passive layer rapture. The slopes of Bode impedance magnitude plots at

intermediate frequencies, S, and the maximum phase angles, $\alpha_{max.}$, deviate from the values of -1 and 90^{o}, respectively. These deviations account for the deviation from ideal capacitive behaviour at intermediate frequencies [39]. Table 3 shows that the values of –S and $\alpha_{max.}$ decrease with the advance of anodic potential. Moreover, the characteristic frequencies of $\alpha_{max.}$ shift to higher values as a result of accelerating the charge transfer processes at more anodic potentials. The gradual departure of -S and $\alpha_{max.}$ from the ideal capacitive values may related to enhancing the rate of passive layer dissolution as a result of its progressive attack as the potential shifts more anodic in the pitting corrosion potential range [40].

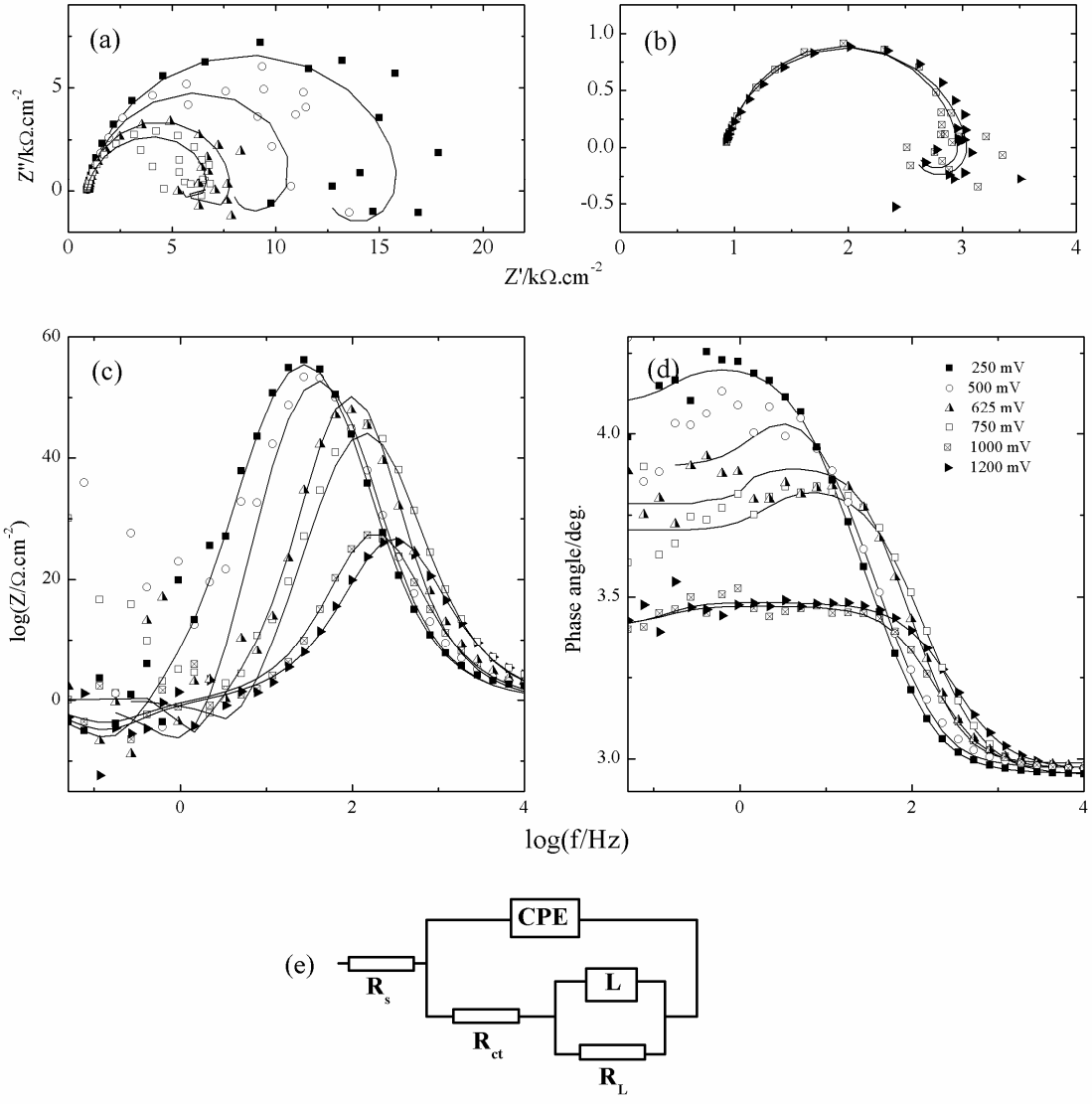

Figure 10. The Nyquist (a, b) and Bode (c, d) plots for tin electrode in 0.1 M acetate solution at different applied potential (e) the equivalent circuit used to fit the EIS data. Dots and lines represent data points and best fits, respectively.

Fig. 11 represents the Nyquist and Bode plots for the tin electrode polarized at 1.0 V in acetate buffers of pH ~ 4.5 and different concentrations. The curves were fitted with the equivalent circuit of Fig. 10e and the fitting parameters were recorded in Table 4. It is clear from these data that R_s has high values at dilute solution. Its value decreases with the solution concentration as a result of increasing the solution conductivity. The observed decrease in the values of R_{ct}, -S and $\alpha_{max.}$ with the solution concentration is related to the formation of weaker passive films and increasing the rate of its pitting dissolution at high concentrations.

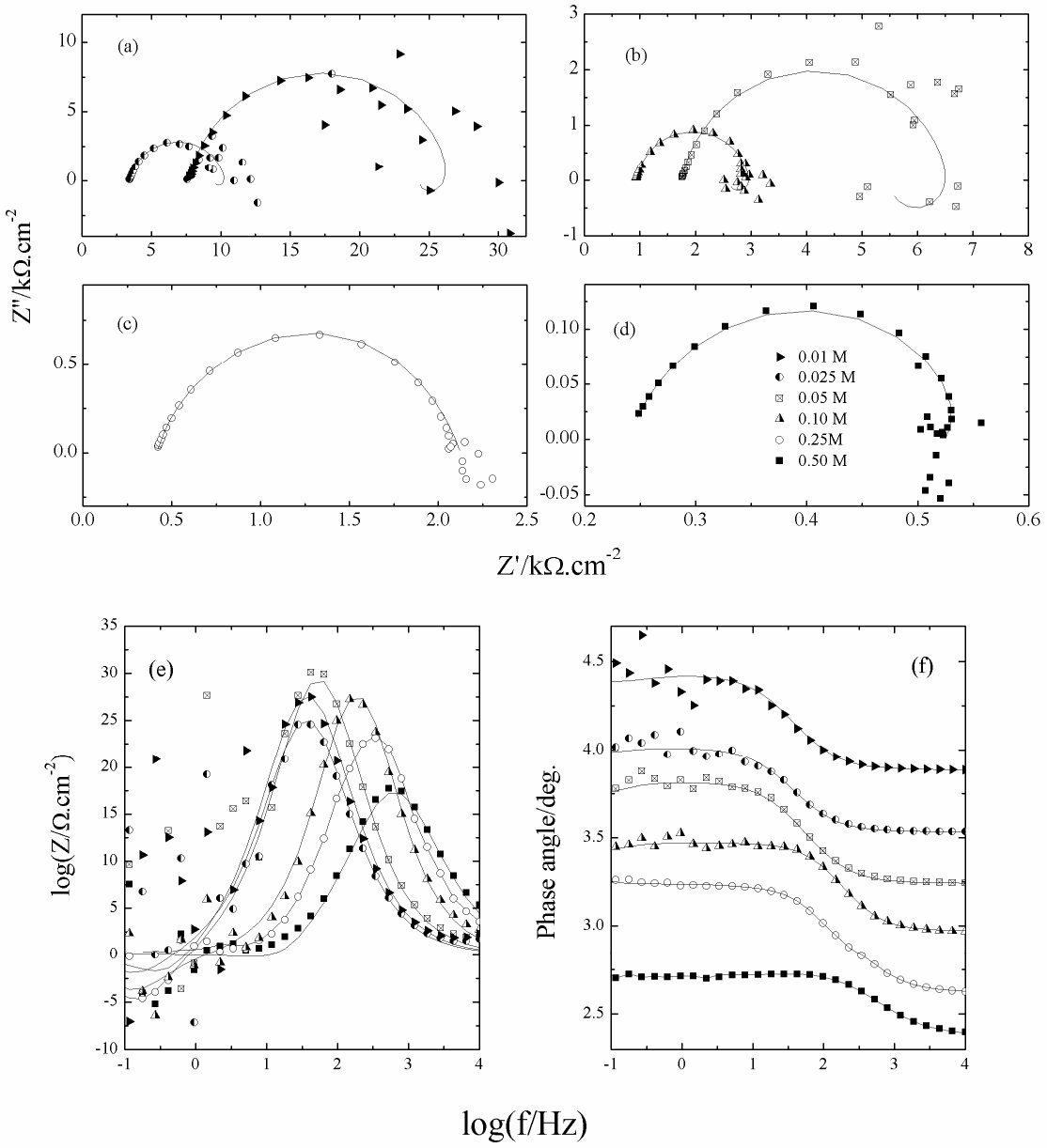

Figure 11. The Nyquist (a-d) and Bode (e, f) plots for tin electrode polarized at 1.0V in acetate buffer solutions with different concentrations. Dots and lines represent data points and best fits, respectively.

Table 3. Electrochemical parameters calculated from EIS measurements on the tin electrode in 0.1 M acetate buffer after 1min of its immersion in the corresponding solution at different applied potentials.

Potential (mV)	R_s (Ω)	Q Y_0 (μF cm^{-2})	n	R_{ct} (Ω)	R_L (Ω)	L/H	-S	$\alpha_{max.}$(deg.)
250	902	0.6019	0.89	11,580	3,990	3,315	0.672	55.81
500	938	0.647	0.92	6,040	3,870	357	0.649	52.76
625	949	0.601	0.98	4,870	2,054	350	0.621	50.31
750	909	0.345	0.90	4.16	1,853	125	0.576	44.04
1000	937	0.399	0.92	1,662	366	395	0.386	27.24
1200	928	0.1678	0.88	1,637	482	530	0.362	26.65

Table 4. Electrochemical parameters calculated from impedance measurements on the tin electrode in acetate buffers with different concentrations (pH 4.5) after 1min of its immersion in the corresponding solution at 1.0 V.

C (M)	R_s (Ω)	Q Y_0 (μF cm^{-2})	n	R_{ct} (Ω)	R_L (Ω)	L/H	-S	$\alpha_{max.}$(deg.)
0.01	7,530	0.104	0.87	16,650	2,465	997	0.331	27.50
0.025	3,420	0.352	0.88	6,110	805	779	0.339	25.20
0.05	1,746	0.382	0.87	3,750	1,089	10^3	0.403	28.14
0.10	937	0.399	0.92	1,662	366	395	0.386	27.10
0.25	413	0.239	0.82	1,710	160	0.695	0.294	23.21
0.50	241	0.350	0.81	287.3	30	0.156	0.232	17.42

4. CONCLUSIONS

The corrosion behavior of tin electrode in acetate buffer solutions was studied by three different techniques. The potentiodynamic voltammetry exhibit two anodic peaks A1 and A2 and three cathodic peaks C1, C2 and C3. This study showed that the corrosion of tin in the potential range of A1 is mixed controlled while in the potential range of A2 is pure diffusion controlled. The action of acetate ion in provoking pitting corrosion is confirmed by light microscope images. Potentiostatic current-time transients were also performed in the potential ranges where pitting corrosion may occur. When the electrode potential shifts to more anodic and solution becomes more concentrated, pits were formed with an increasing nucleation rates and decreasing growth rates. Impedance measurements confirms the pitting corrosion and the existence of adsorbed species on the tin surface in the potential ranges around E_{pit}. It confirms also the formation of weaker tin passive layers in acidic acetate solutions with higher concentration and/or at more anodic potentials

References

1. E. E. F. El-Sherbini, *J. Electroanal. Chem.*, 584 (2005) 167 and references cited therin.
2. S.S. Abd El-Rehim, H.H. Hassan and N.F. Mohamed, *Corros. Sci.*, 46 (2004) 1071.

3. S. S. Abdel Rehim, S. M. Sayyah and M. M. El Deeb, *Mater. Chem. Phys.*, 80 (2003) 696.
4. C.M.V. Almeida and B.F. Giannetti, *Mater. Chem. Phys.*, 69 (2001) 261 and references cited therin.
5. C.M.V. Almeida, B.F. Giannetti and T. Rabockai, *J. Appl. Electrochem.*, 29 (1999) 123.
6. S. S. Abd El Rehim, A. M. Zaky and N. F. Mohamed, *J. Alloys Compd.*, 424 (2006) 88.
7. K. Ogura, Electrochim. Acta, 25 (1980) 335.
8. A.E. Smith, Analist., 98 (1973) 209.
9. F.A. Cotton and G. Wilkinson, *Advanced Inorganic Chemistry*, third ed., Interscience–Wiley, New York, (1972).
10. J.L. Crolet and M. Bonis, *NACE Corrosion 83*, Houston, Paper 160, 1983.
11. J.L. Crolet, N. Thevenot and A. Dugstad, *NACE Corrosion 99*, San Antonio, Paper 24, 1999.
12. W.M. Hedges and L. McVeigh, *NACE Corrosion 99*, San Antonio,Paper 21, 1999.
13. M. A. Veloz and I. González, *Electrochim. Acta*, 48 (2002) 135.
14. Y. Garsany, D. Pletcher and B. Hedges, *J. Electroanal. Chem.*, 538-539 (1984) 285.
15. W. J. Albery and R. P. Bell, *Proc. Chem. Soc.*, (1963) 169.
16. Lj. Vracar and D. M. Drazic, *J. Electroanal. Chem.*, 339 (1992) 269.
17. S-I. Pyun and S-M. Moon, *J. Solid State Electrochem.*, 3 (1999) 331.
18. Z. Szklarska–Smialowska, *Pitting Corrosion of Metals*, NACE, Houston,TX, 1986.
19. H. H. Hassan, *Electrochim. Acta*, 51 (2005) 526.
20. H. H. Hassan, *Electrochim. Acta*, 52 (2006) 5966.
21. T. Berzins and P. Delahay, *J. Am. Chem. Soc.*, 75(1953) 555.
22. W. Müller, *Trans. Faraday Soc.*, 27 (1931) 737.
23. A.J. Calandra, N. R. Tacconi, R. Pereiro and A. J. Arvia, *Electrochim. Acta*, 19 (1974) 901.
24. M. Metikos–Hukovic and I. Milosev, *J. Appl. Electrochem.*, 22 (1992) 448.
25. C.Y. Chao, L.F. Lin and D.D. Macdonald, *J. Electrochem. Soc.*, 128 (1981) 1187.
26. D.D. Macdonald and M.J. Urquidi-Macdonald, *J. Electrochem. Soc.*, 137 (1990) 2395.
27. J.C. Nelson and R.A. Oriani, *Electrochim. Acta*, 35 (1990) 1719.
28. I.Milosev and M. Metikos-Hukovic, *J. Electrochem. Soc.*, 138 (1991) 61.
29. H.J. Engell and D.N. Stolica, *Z. Phys. Chem. Unterr.*, 20 (1959) 113.
30. M. A. Amin, S. S. Abd El-Rehim, E. E. F. El-Sherbini and R. S. Bayyomi, *Electrochim. Acta*, 52 (2007) 3588.
31. H. J. W. Lenderrink, M. V. D. Linden and J. H. W. De Wit, *Electrochim. Acta*, 38 (1993) 1989.
32. M. Kedam, O.R. Mattos and H. Takenouti, *J. Electrochem. Soc.*, 128 (1981) 257.
33. E. M. Sherif and S.-M. Park, *Electrochim. Acta*, 51 (2006) 1313.
34. A.H. Moreira, A.V. Benedetti, P.T.A. Sumodjo, J.A. Garrido and P.L. Cabot, *Electrochim. Acta*, 47 (2002) 2823.
35. M.S. Abdelaal and M.S. Morad, *Br. Corros. J.*, 36 (2001) 253.
36. P. Bommersbach, C. Alemany-Dumont, J. P. Millet and B. Normand, *Electrochim. Acta*, 51 (2005) 1076.
37. F. Mansfeld, Corrosion 36 (1981) 301; *Corrosion*, 38 (1982) 570.
38. A.V. Benedetti, P. T. A. Sumodjo, K. Nobe, P. L. Cabot and W. G. Proud, *Electrochim. Acta*, 40 (1995) 2657.
39. H. H. Hassan, M. A. Amin, S. Gubbala and M.K. Sunkara, *Electrochim. Acta*, 52 (2007) 6929.
40. H. H. Hassan, *Electrochim. Acta*, (2007), doi:10.1016/j.electacta.2007.08.021.